

# Slow Crystallization Kinetics of Poly(vinyl alcohol) in Confined Environment during Cryotropic Gelation of Aqueous Solutions

Finizia Auriemma,\* Claudio De Rosa, and Roberto Triolo

*Dipartimento di Chimica, Università di Napoli Federico II, Complesso Monte Sant' Angelo, Via Cintia, 80126 Napoli, Italy, and Dipartimento di Chimica Fisica "Filippo Accascina", Università degli Studi di Palermo, Viale delle Scienze, Ed. 17, 90128 Palermo, Italy*

*Received August 24, 2006; Revised Manuscript Received October 2, 2006*

**ABSTRACT:** The gelation kinetics of aqueous solutions of poly(vinyl alcohol) (PVA) during freezing at  $-13\text{ }^{\circ}\text{C}$  has been investigated with time-resolved small angle neutron scattering. Crystallization of PVA takes place inside an unfrozen liquid microphase that forms in the matrix of ice crystals and follows a first-order kinetics during the early stages and becomes very slow in the later stages with an apparent Avrami exponent lower than 1. Crystallization of PVA at low temperatures is responsible of formation of strong physical gels upon defrosting, provided that the concentration of PVA is higher than a critical value.

## Introduction

The possibility of obtaining strong physical gels by cryogenic treatments of aqueous poly(vinyl alcohol) (PVA) solutions is well-known since the 1970s.<sup>1,2</sup> The cryogenic treatment basically consists of freezing an initially homogeneous polymer solution at low temperatures, storing in the frozen state for a definite time, and defrosting. Freezing is generally performed at high cooling rates and, in order to improve the strength of the gels, freezing and thawing are repeated a number of times. The strength of PVA cryogels prepared by means of freeze/thaw cycles depends on the initial polymer concentration in the solution to be frozen, the thawing rate, the permanence time of the solution at low temperatures, and the number of imposed freeze/thaw cycles, whereas it is rather independent of the temperature of freezing and the cooling rate of the initial solution to that temperature.<sup>1b,3</sup> Strong physical gels may be obtained by imposing a single freeze/thaw cycle either with use of slow thawing rates or by the prolonged storage of the samples at "high" subzero temperatures.<sup>3</sup> In any case, for the solutions with PVA concentration of practical interest, freezing temperatures below  $-10\text{ }^{\circ}\text{C}$  are required to induce crystallization of water, formation of fine ice crystals, and of a macroscopic gel upon thawing.<sup>1</sup>

At variance with physical gels obtained by more conventional techniques, hydrogels obtained by repeatedly freezing and thawing water/PVA solutions show a porous structure, high modulus, rubber elasticity, and are mechanically stable over a large range of temperatures. These properties, along with lack of toxicity, biocompatibility, and large water content, make freeze/thaw PVA hydrogels attractive matrices for chromatography and hosts for biological nanoparticles.<sup>1</sup>

The physical gelation of aqueous solutions of PVA at temperatures above the crystallization of water may involve several processes, namely phase transitions (polymer crystallization and/or liquid–liquid phase separation), hydrogen bonding, and entanglements.<sup>4</sup> According to Komatsu et al.,<sup>5</sup> the phase diagram of PVA/water binary system shows an upper critical solution temperature in which the spinodal curve crosses the sol–gel transition curve. Gelation takes place both below and

above the spinodal curve, indicating that gels may be formed either accompanied by spinodal decomposition<sup>6–8</sup> or without liquid–liquid phase separation, respectively. In both cases, PVA crystallites act as knots of the network. The distribution of crosslinks in these kinds of gels is rather uniform, resulting in gels with a homogeneous morphology.<sup>8</sup>

Cryotropic gelation of moderately diluted PVA solutions produces heterogeneous materials with essentially different morphology compared to more conventional gels obtained from nonfrozen systems.<sup>1</sup> The main characteristic feature of PVA cryogels is a network including interconnected micro- and macropores.<sup>1,2,9,10</sup> It has been shown that this porous structure is imprinted during the early freezing of the originally homogeneous solution by formation of ice crystals due to the fact that the crystallization of water is not complete, but an unfrozen liquid microphase, consisting of a water solution more concentrated in PVA than the initial solution, remains present even for a prolonged time at low temperatures.<sup>1b</sup> The gel network is formed in this microphase so that, when ice crystals melt upon thawing the system, they leave macropores filled by solvent. The gels formed upon defrosting are rather strong and able to include up to 90% in mass of water. The tie points of the macroscopic network are essentially PVA crystallites connected by portions of chains swollen by the solvent. Therefore, PVA gels formed at temperature below the crystallization temperature of water not only include large pores but also micropores in between the polymer chains constituting a swollen amorphous phase.<sup>1,9</sup> The heterogeneous structure of these gels may be described, in the long range, in terms of two bicontinuous phases, consisting of polymer-rich and polymer-poor regions.<sup>1,10</sup> The polymer-rich regions have average dimensions on the order of microns<sup>1</sup> and include crystallites of PVA of size of 3–4 nm<sup>11,12</sup> and a swollen amorphous phase, the average distance between crystallites being on the order of 10–20 nm.<sup>10</sup> The polymer-poor regions, in turn, allow almost unhindered diffusion of large and small molecules and have a size of hundreds nanometers.<sup>1,2</sup>

The size and amount of PVA crystalline aggregates in freeze/thaw PVA hydrogels play an important role in their performances in application because the dimensional stability, toughness, strength to external stresses, and thermal stability of PVA cryogels are critically dependent on these parameters.<sup>1,12</sup> It has

\* Corresponding author. E-mail: finizia.auriemma@unina.it. Telephone: ++39 081 674341. Fax ++39 081 674090.

been shown that PVA crystallites are formed already during the first freeze/thaw cycle<sup>1,9</sup> and that this crystalline form corresponds to the monoclinic form with chains in a trans-planar conformation,<sup>1,12</sup> studied by Bunn.<sup>13</sup> The amount of crystalline fraction lies in the range 0.4–5%, dependent on the sample history, and increases with increasing the aging time at room temperature,<sup>9,12</sup> the time the sample is kept at subzero temperatures,<sup>1</sup> the number of freeze/thaw cycles, and the concentration of the initial PVA solution used for the preparation of the gel.<sup>12</sup> The comprehension of the factors that govern the cryogelation mechanism of PVA homogeneous solutions and, in particular, the crystallization of PVA in these heterogeneous systems, may allow controlling the final architecture of the cryogel by simply tuning the conditions of preparation, with the aim of obtaining materials with enhanced properties for tailored applications.

The number and kinds of processes subtending the cryotropic gelation of PVA/water solutions are still unclear. In particular, it is not yet clear whether PVA crystallites form already at subzero temperatures during the first freezing step or during the thawing and successive aging time at room temperature. It has been suggested that crystallization of PVA in the unfrozen liquid microphase plays a fundamental role in the formation of these gels.<sup>1b</sup> On the basis of the phase diagram by Komatsu et al.,<sup>5</sup> below 0 °C, solutions of PVA having the typical concentrations used for preparation of cryogels should be below the spinodal curve. Because at temperatures below 0 °C the water crystallizes, the gelation process may involve two concomitant and at the same time competitive phenomena: crystallization of PVA due to eutectic-like behavior and spinodal decomposition.<sup>6–8</sup> A further complication arises due to the fact that, although the glass transition temperature of dry PVA at 85 °C decreases significantly in the presence of water,<sup>1a</sup> at temperatures generally used for preparation of freeze/thaw PVA hydrogels, i.e., below –10 °C, the mobility of chains should be strongly reduced.

In this article, the sol–gel transition of aqueous solutions of PVA during freezing is investigated for the first time using time-resolved small angle neutron scattering (SANS), with the aim of obtaining simultaneous information concerning the gelation mechanism and the kinetics of formation of PVA aggregates responsible for the development of a stable gel network. SANS measurements reflect, indeed, microstructural changes on the length scales from one to hundreds nanometers that are particularly relevant to the development of the complex structure of freeze/thaw PVA hydrogels and allows obtaining information that is not easy to obtain using more conventional techniques, for instance wide-angle X-ray diffraction, because the degree of crystallinity reached by PVA is very low,<sup>1,12</sup> and the Bragg's reflections due to PVA crystals would be buried by the scattering from water.

## Experimental

Two solutions with PVA concentration of 5% and 10% mass/mass have been studied. They have been obtained by dissolving atactic PVA (Aldrich, ref 36, 315-4, mass average molecular mass of about 115 000, degree of hydrolysis 98–99%) in deuterated water (Aldrich, stated purity 99.8%) at 96 °C, under reflux and stirring. In both cases, a homogeneous solution has been obtained that does not gellify even after 1 month when kept at room temperature in sealed vials in order to prevent water evaporation.

SANS measurements of solutions have been performed at the KWS2 facility located at the Forschungszentrum of Jülich. Solutions have been placed in 2 mm path length Hellma quartz cells. Neutrons with an average wavelength  $\lambda$  of 0.7 nm and a wavelength spread  $\Delta\lambda/\lambda \leq 0.2$  have been used.

Measurements have been performed using a two-dimensional array detector at sample-to-detector distance of 4 m. This config-

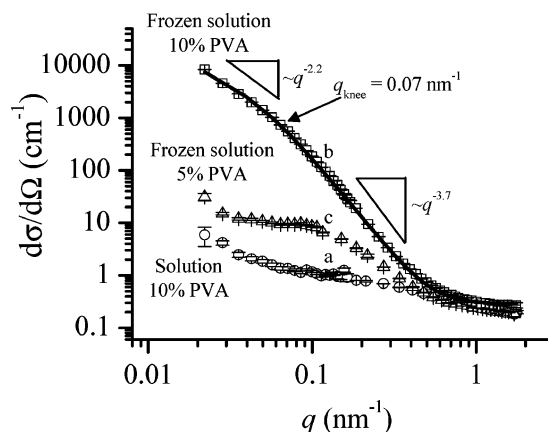


**Figure 1.** Comparison of the SANS data recorded from 10% PVA in solution at room temperature (a, ○), in the frozen system after 390 min at –13 °C (b, □), and from 5% PVA in the frozen solution after 160 min at –13 °C (c, △). The solid line b is the fit of experimental data from the 10% PVA solution in the frozen state to a hierarchical structural model<sup>16</sup> given by the product of eqs 1 and 2 (see the text).

uration allows collecting the scattered neutrons in the range of scattering vector  $q (= 4\pi \sin\theta (\lambda)^{-1})$  comprised between 0.1 and 0.9 nm<sup>–1</sup>.

Measurements have been started immediately after quenching the solutions from room temperature to a precooled thermostatic bath at –13 °C. The temperature control of thermostatic bath was  $\pm 1^\circ\text{C}$ . The time of each measurement has been set equal to 36 s, and the structural transformations of solutions have been followed for at least 1 h. SANS data at sample-to-detector distance of 2, 4, and 20 m have been also collected from the initial solutions at room temperature and the fully frozen systems in the range  $0.02 < q < 1.2 \text{ nm}^{-1}$ . Reproducibility of data has been checked by repeating the experiments on at least two different solutions with the same PVA concentration.

Raw data have been corrected for electronic background and empty cell scattering. Detector sensitivity corrections and transformation to absolute scattering cross sections  $(d\sigma/d\Omega)(q)$  have been made with a secondary Lupolene standard. Data were then radially averaged, and absolute scattering cross sections were obtained.

## Results and Discussion

The SANS patterns from 10% PVA in the initial solution and in the frozen system and from 5% PVA in the frozen solution are compared in Figure 1. As shown in a previous study,<sup>10</sup> the shape of the SANS curve of the initial solution for  $q > 0.05 \text{ nm}^{-1}$  is apparently similar to that from a collection of Gaussian polymer coils (curve a of Figure 1). However, the upturn of curve a of Figure 1 for  $q < 0.04 \text{ nm}^{-1}$  indicates that the solution may not be treated as a diluted or semidiluted solution, in agreement with the fact that the concentrations of our solutions are well above the overlap concentration  $c^*$ . The overlap concentration may be evaluated as the ratio  $c^* = M/(VN_A)$ , with  $M$  the molecular mass of PVA,  $N_A$  the Avogadro number,  $V \approx R_g^3$ , the volume of solution spanned by the polymer chain, i.e., the so-called pervaded volume, and  $R_g$  the gyration radius of PVA.<sup>14</sup> In fact, because the density of D<sub>2</sub>O at room temperature is 1.112 g/cm<sup>3</sup>, assuming that the density of PVA is 1.3 g/cm<sup>3</sup> (the densities of amorphous<sup>1</sup> and crystalline<sup>13</sup> PVA correspond to 1.269 and 1.348 g/cm<sup>3</sup>, respectively) and a value of  $R_g$  equal to 16.3 nm (as determined by Nagy<sup>15</sup> by size exclusion chromatography for water solutions of a PVA sample with 98% hydrolysis and  $M_w = 110\,000$ ), the overlap concentration of PVA in water corresponds to  $c^* = 0.018 \text{ g/cm}^3$  and therefore to  $\sim 1\%$  PVA by weight. However, the fact that the 10% and 5% PVA solutions are stable and remain transparent

and homogeneous, even for a long time when kept at room temperature in sealed vials in order to prevent water evaporation, rules out that the gel that is formed by cryogenic treatment is partly already formed at room temperature before the cooling of the solution at subzero temperatures.

From Figure 1, it is apparent that the scattering cross section from the 10% PVA solution increases upon freezing and exhibits two distinct regimes in  $q$  values, separated by a knee located at  $0.07 \text{ nm}^{-1}$  (curve b, squares, in Figure 1). The scattered intensity decays as approximately  $q^{-3.7}$  at high  $q$  values ( $0.07 \text{ nm}^{-1} < q < 0.35 \text{ nm}^{-1}$ ) and as  $q^{-2.2}$  at low  $q$  values ( $0.02 < q < 0.07 \text{ nm}^{-1}$ ). This indicates that the 10% PVA frozen solution is nonuniform, being characterized by the presence of large heterogeneities dispersed within the ice matrix. We assume that the nonuniform structure of the frozen system is due to the presence of the unfrozen liquid microphase, whose characteristic size,  $L(\approx 2\pi/q_{\text{knee}})$ , is approximately equal to 85–90 nm.

The  $q^{-2.2}$  power law dependence of SANS intensity in scattering vector at low  $q$  values shown by the 10% PVA frozen solution (curve b in Figure 1) probably reflects a self-similar fractal nature of the system. It indicates that the unfrozen liquid microphase does not form isolated droplets scattering independently, but that these droplets form clusters of dimensions larger than 300 nm in the matrix of ice crystals. This hypothesis is supported by the fact that the SANS curve from the 10% PVA frozen solution (curve b of Figure 1) is quite different from that of the 5% PVA frozen solution (c in Figure 1). Also, in the frozen system with 5% PVA, crystallization of water is incomplete, but in this case, the unfrozen liquid microphase forms more isolated droplets having a uniform distribution in the matrix of ice. It is worth noting that, whereas the more concentrated solution of PVA gives rise to a gel upon thawing, the 5% PVA solution is unable to form a macroscopic gel upon the same freeze/thaw treatment. In other terms, for polymer concentrations below a critical value, the total volume of the unfrozen liquid microphase is too low, preventing the clustering process of the droplets with consequent formation of interconnected macroscopic network. The clustering process of the droplets, in turn, plays a key role in the formation of the gel. When this process is prevented by the low polymer concentration of the solution, the system does not undergo gelation.

For the 10% PVA frozen solution, the size of the primary particles ( $L$ ) constituting the network of the unfrozen liquid microphase and the power law dependences in  $q$  of the scattering cross section aside the knee found empirically from SANS data are close to those found through the fit of the experimental SANS data (points b in Figure 1) to a hierarchical structural model that takes into account the existence of a network of fractal aggregates of size  $\xi$  formed by monodisperse primary objects of spherical shape of radius  $r (= L/2)^{16}$  (the fitting curve is indicated by the solid line in b of Figure 1). The scattering cross section is assumed proportional to the product of the form factor  $P(q)$  (eq 1) relative to a single primary scattering object and the structure factor  $S(q)$  (eq 2) that reflects the degree of order of primary objects within the aggregates:

$$P(q) = \left(1 + \frac{\sqrt{2}}{3} q^2 r^2\right)^{(D_s-1)/2} \quad (1)$$

$$S(q) = 1 + \frac{D\Gamma(D-1)}{(q\xi)^D} \left(1 + \frac{1}{(qr)^2}\right)^{(1-D)/2} \quad (2)$$

In eq 1,  $D_s$  is the dimensionality of the interfacial region of the primary objects of radius  $r$ , constituting the unfrozen liquid

microphase, and determines the power law dependence of the scattering cross section at a large scattering vector, whereas in eq 2,  $\Gamma$  is the gamma function and  $D$  describes how the cluster mass scales with the cluster size ( $M \propto \xi^D$ ) and therefore determines the power law exponent of the scattering cross of the fractal aggregates ( $S(\xi^{-1} < q < r^{-1}) \propto q^{-D}$ ). The fit of experimental data from the 10% PVA frozen system to the above-described hierarchical structural model gives  $D_s = 3.67 \pm 0.04$ ,  $r = 45.6 \pm 0.1 \text{ nm}$ , and  $D = 2.19 \pm 0.01$ . It is worth noting that our SANS data do not allow a direct determination through the fitting procedure of the  $\xi$  value. In fact, at  $q$  values lower than  $2\pi/\xi$ , the scattering cross section of our system is expected to be high and with a tendency to level off; in other words, neutrons should probe length scales at which the system does no longer show any inhomogeneities, and therefore it cannot be resolved. However, we have no indication of leveling off at low values of  $q$  in curve b of Figure 1, probably because  $\xi$  is greater than  $2\pi/q_{\text{min}}$ ,  $q_{\text{min}}$  being the lowest value of  $q$  experimentally achieved. In these cases, in the fitting procedure,  $\xi$  can be fixed to a value high enough not to produce any effect on the values of the fitting parameters  $D_s$ ,  $r$ , and  $D$  in the measurable range of  $q$ .

It is worth noting that the scattering cross section from the 10% PVA frozen solution decays approximately as  $q^{-4}$  ( $D_s \approx 4$ ) at high  $q$  values (curve b of Figure 1), indicating that, on the length scale of 10–100 nm, heterogeneities are present that obey Porod's law, i.e., they are separated by nearly sharp boundaries. This length scale is particularly relevant to the formation of a network structure in the unfrozen liquid microphase, where the crosslinks are ensured by the presence of PVA crystallites,<sup>1,2</sup> separated from the surrounding solution by sharp boundaries.

In order to investigate the structural transformations occurring in the unfrozen liquid microphase, we have collected SANS data in the  $q$  range between 0.1 and  $0.9 \text{ nm}^{-1}$  during the permanence of 10% and 5% PVA solutions at  $-13^\circ\text{C}$  (Figure 2). It is apparently a gradual increase of scattering cross section during the treatment at  $-13^\circ\text{C}$ , which is more pronounced for the 10% than for the 5% PVA system.

The increase of the scattering cross sections from PVA solutions during the permanence time at  $-13^\circ\text{C}$  may not be due to the crystallization of water, which takes place in the first 6 min (as indicated by DSC analysis). In this  $q$  range, the contribution of  $\text{D}_2\text{O}$  should be very low. The data of Figure 2 reflect microstructural changes that occur on the length scale between  $2\pi/0.9$  and  $2\pi/0.1 \text{ nm}$ , involving the formation of heterogeneities inside the unfrozen liquid microphase, giving rise to a microgel network where the crosslinks are PVA crystallites. In fact, because the unfrozen liquid microphase consists of a  $\text{D}_2\text{O}$ /PVA solution more concentrated in PVA than the initial homogeneous solution used for the experiments, most likely the structural changes are driven by aggregation phenomena of PVA chains via hydrogen bonding, with consequent formation of crystalline or precrystalline aggregates. In addition, as discussed above, these microheterogeneities, i.e., the PVA crystallites, would be separated from the surrounding solution by rather sharp boundaries.

The hypothesis that crystallization of PVA takes place inside the unfrozen liquid microphase during the permanence time of the solution at subzero temperatures is in agreement with the results of previous investigations performed using SANS<sup>10</sup> and SAXS<sup>9</sup> techniques on PVA hydrogels obtained by imposing a different number of freeze/thaw cycles (from 1 to 12 cycles). These investigations<sup>9,10</sup> have indicated that the scattering cross



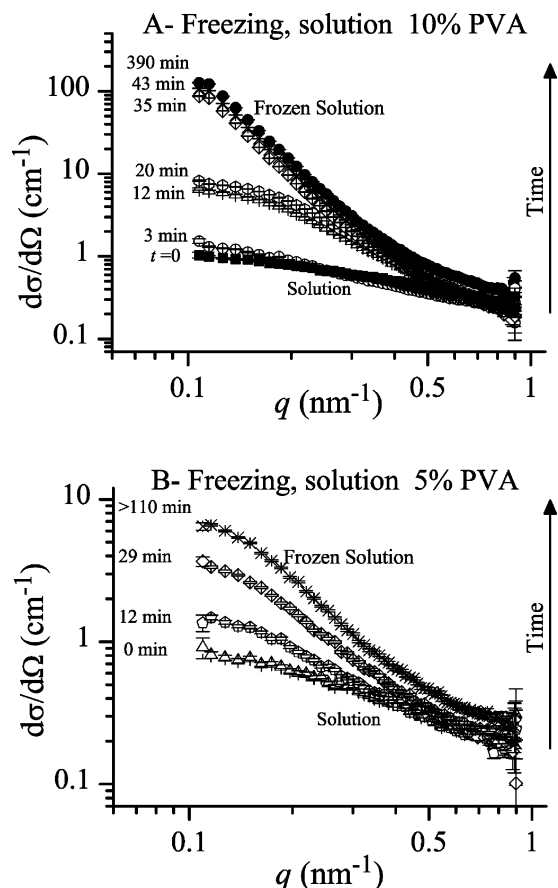


**Figure 2.** SANS curves from the 10% (A) and 5% (B) PVA solutions during freezing at  $-13\text{ }^{\circ}\text{C}$ . The permanence time (min) of solutions at  $-13\text{ }^{\circ}\text{C}$  is indicated.

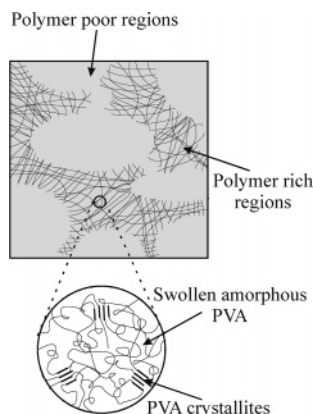


**Figure 3.** Model of the bicontinuous structure of PVA hydrogels obtained by freeze/thaw cycles with a PVA-rich phase and a PVA-poor phase. The microgel fraction that forms in the unfrozen liquid microphase at subzero temperatures during the first freezing of the solution acts as a building block to form the network structure in the polymer-rich regions.

section of these gels in the  $q$  range between  $0.09$  and  $1.2\text{ nm}^{-1}$  reflects heterogeneities associated with the presence of a swollen amorphous phase and PVA “crystallites”, fringed micelle like, of average dimensions of  $3\text{--}4\text{ nm}$ , placed at distance of  $10\text{--}20\text{ nm}$ . In particular, the SANS investigation of ref 10 indicates that the swollen amorphous phase and the crystals are formed in polymer-rich regions intermingled with polymer-poor regions to form two bicontinuous phases. The macroscopic network in these gels is ensured by the PVA chains belonging to the swollen amorphous phase connecting the PVA crystallites.<sup>9,10</sup> A model of the bicontinuous structure of freeze/thaw PVA hydrogels is

shown in Figure 3. Probably, the polymer-rich regions of these gels originate from the unfrozen liquid microphase that forms during the first freezing of the initial homogeneous solution at subzero temperatures.

The change of SANS intensity with respect to the initial homogeneous solution as a function of time has been analyzed using the scattering invariant in the working hypothesis that, during the treatment at  $-13\text{ }^{\circ}\text{C}$ , the scattering pattern contains additive contributions from the aggregated and not aggregated phases that form in the unfrozen liquid microphase. More precisely, we have evaluated the excess of scattering invariant at time  $t$  with respect to the scattering invariant of the initial solution (at time  $t = 0$ ) (normalized to the volume fraction of PVA in each solution,  $\Phi_{\text{PVA}}$ ), defined by the following equation:

$$\Psi(t) = \frac{\int_{q_{\min}=0.1}^{q_{\max}=0.9} q^2 \left\{ \left[ \frac{\partial \sigma}{\partial \Omega}(q) \right]_t - \left[ \frac{\partial \sigma}{\partial \Omega}(q) \right]_{t=0} \right\} dq}{\Phi_{\text{PVA}}} \quad (3)$$

Within this framework, the integrated function given by eq 3, for an ideal two-phase system, is proportional to the volume fraction of aggregates (for small values) and is not sensitive to the structure.<sup>17</sup> In fact, during the permanence time of the solutions at  $-13\text{ }^{\circ}\text{C}$ , the scattering cross section for  $q$  less than  $0.1\text{ nm}^{-1}$ , after completion of the crystallization of the water, is not expected to be greatly affected by formation of the network structure inside the unfrozen liquid microphase because these microstructural changes occur at a length scale less than  $2\pi/0.1\text{ nm}$ . Therefore, the extension of the integral in eq 3 to  $q = 0$  would add a constant term, which does not affect our kinetic analysis, whereas its extension from  $q = 0.9\text{ nm}^{-1}$  up to infinity would be negligible.

The reduced scattering invariant obtained from SANS measurements in the  $q$  range  $0.1\text{--}0.9\text{ nm}^{-1}$  of Figure 2 for the 5% and 10% PVA solutions is reported in Figure 4A as a function of permanence time of the solutions at  $-13\text{ }^{\circ}\text{C}$ . In both cases, the reduced scattering invariant shows a smoothed S shape, and does not reach a plateau value, even for prolonged times of permanence of the systems at  $-13\text{ }^{\circ}\text{C}$ . The reduced scattering invariant of 5% and 10% PVA solutions during the treatment at  $-13\text{ }^{\circ}\text{C}$ , indeed, increases smoothly in the first 30 min, presents a clear upturn around 30–40 min, and increases smoothly again in the successive 120–330 min of freezing.

This suggests the hypothesis that, after completion of the crystallization of the solvent at  $-13\text{ }^{\circ}\text{C}$  (taking less than 6 min), the PVA chains that are mostly segregated in the unfrozen liquid microphase tend to form precrystalline or crystalline aggregates, probably because the concentration of the liquid microphase reaches a critical value. However, the full crystallization of PVA may not be complete and is slowed down due to the fact that the unfrozen liquid microphase gellifies, preventing the attainment of thermodynamic equilibrium, which should involve only two-phases, ice crystals, and PVA crystallites. The formation of the gel in the microphase may be determined by aggregation of PVA chains in a confined environment, driven by hydrogen bonding and consequent formation of crystallites, and vitrification of the swollen amorphous phase at temperature, which is likely below the glass transition.<sup>1a</sup>

The data of Figures 2 and 4A provide direct evidence that the structure of the supramolecular aggregates entering into the composition of such a microgel fraction are namely PVA crystallites. Crystallization of PVA within the unfrozen liquid microphase with successive formation of a gel microphase probably occurs also in the case of the solution with 5% PVA, during the freezing treatment at  $-13\text{ }^{\circ}\text{C}$ , even though the relative

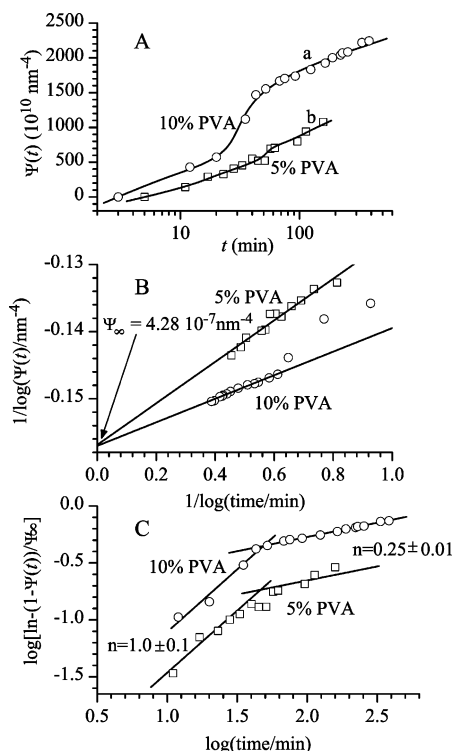


**Figure 4.** (A) Reduced scattering invariant,  $\Psi(t)$  (eq 3), as a function of time during the treatment at  $-13\text{ }^{\circ}\text{C}$  for 10% (a) and 5% (b) PVA solutions.  $\Psi(t)$  is calculated from the SANS data of Figure 2. (B) Extrapolation of reciprocal of logarithmic scattering invariant,  $[\log(\Psi(t))^{-1}]$ , with respect to reciprocal logarithmic time,  $[\log(t)]^{-1}$ , of PVA solutions at different concentrations, at  $[\log(t)]^{-1} = 0$ , to find the scattering invariant at infinite time,  $\Psi_{\infty}$ . (C) Avrami plot of the reduced scattering invariant normalized to the values of  $\Psi_{\infty}$  of PVA solutions at different concentrations.

amount of gel microphase is too low to give rise to an interconnected macroscopic gel network, preventing the formation of a macroscopic gel upon thawing.

The kinetics of microstructural transformations in the unfrozen liquid microphase from the PVA solutions with 5 and 10% PVA evaluated from SANS measurements of Figure 2 has been analyzed using the Avrami equation:

$$1 - \Psi(t)/\Psi_{\infty} = \exp(-kt^n) \quad (4)$$

In eq 4,  $\Psi_{\infty}$  is the value of the reduced scattering invariant reached by the solutions during the permanence at  $-13\text{ }^{\circ}\text{C}$  at infinite time, and the ratio  $\Psi(t)/\Psi_{\infty}$  represents the extent of gelation in the unfrozen liquid microphase. Because the crosslinking process that gives rise to the formation of the gel network in the unfrozen liquid microphase is PVA crystallization, the Avrami analysis using the parameter  $\Psi(t)/\Psi_{\infty}$  allows finding the exponent  $n$  that governs the crystallization kinetics of PVA during the gelation.

A common value of  $\Psi_{\infty} = 4.28 \times 10^{-7} \text{ nm}^{-4}$  may be obtained for both solutions by linear extrapolation of the reciprocal of the logarithmic scattering invariant with respect to reciprocal logarithmic time (Figure 4B). This indicates that the extent of gelation in the unfrozen liquid microphase reaches a value of  $\approx 50\%$  for the 10% PVA solution after 390 min at  $-13\text{ }^{\circ}\text{C}$  and of  $\approx 20\%$  for the 5% PVA solution after 160 min at  $-13\text{ }^{\circ}\text{C}$ .

The Avrami exponent obtained from the linear fits in Figure 4C is for both solutions  $n = 1$  in the first 40 min and  $n = 0.25$  during the successive minutes. It is worth noting that the extrapolated value of  $\Psi_{\infty}$  is an upper limit, and a change of

$\Psi_{\infty}$  value of 20–30% does not affect very much the values of  $n$  (maximum variations being of 10–15%). This means that the determination of  $\Psi_{\infty}$  is relatively insensitive to the kinetics.

An exponent of  $n = 1$  is consistent with one-dimensional (fibrillar) growth mechanism controlled by heterogeneous (athermal) nucleation.<sup>18</sup> Athermal nucleation is triggered by the active surface of ice at the interface between the ice matrix and the unfrozen liquid microphase. The low Avrami exponent of 0.25 in the later stages of crystallization kinetics of PVA is rather uncommon. Surprisingly low values of Avrami exponents have been found also in the case of kinetics involving crystallization of the crystalline forms stable at high temperatures of trans-1,4-polybutadiene and polytetrafluoroethylene,<sup>19</sup> characterized by a high degree of conformational disorder and of rigid copolyesters of 1,4-dihydroxybenzoic acid and 2,6-dihydroxynaphthoic acid.<sup>20</sup> According to Cheng,<sup>20</sup> a simple explanation of Avrami exponents lower than 1 may be a decrease in the linear crystal growth rate,  $v$ , as crystallization proceeds, contrary to the assumptions of Avrami treatment that the growth rate depends only on the temperature and not on the time. In the hypothesis that  $v$  scales as  $t^m$ , with  $m$  a negative exponent, the application of Avrami theory still holds in these cases, but the measured exponent  $n$  should be divided by a factor  $m + 1$  in order to give the correct Avrami dimensionality for the growth of crystals (see ref 20). There are many mechanisms that can alter the linear growth rate; for instance, in a diffusion controlled transition, the growth rate would scale as  $t^{-0.5}$ . In our case, a possible reason for  $m < 0$  and thus for a lower apparent coefficient  $n$  may be restriction of crystal growth due to the fact that previously formed PVA crystals reduce the mobility of PVA chains dissolved in the unfrozen liquid microphase. This reduced mobility, in turn, results in the gellification of the unfrozen microphase. For the more diluted PVA solution, our data indicate that crystallization of PVA probably also takes place, even though a macroscopic gel is not formed upon defrosting due to the fact that the relative amount of gel microphase is too low to give rise to an interconnected macroscopic gel network at subzero temperatures.

## Concluding Remarks

In this paper, we provide conclusive evidence that crystallization of PVA in the unfrozen liquid microphase, during the permanence of the solutions at low temperatures, plays a key role in the formation of PVA hydrogels by freeze/thaw technique.

It is clearly shown that upon freezing an initially homogeneous PVA solution at low temperatures, the formation of ice crystals induce a progressive increase of the concentration of PVA in the surrounding solution, up to reaching a critical composition. This solution constitutes the so-called unfrozen liquid microphase. In these small regions, whose size is on the order of 80 nm, crystallization of PVA takes place. However, although the temperature of the system is likely below the eutectic temperature, the crystallization of PVA may not be complete because the unfrozen liquid microphase gellifies, preventing the attainment of thermodynamic equilibrium. Crystallization of PVA follows a first-order kinetics during the early stages and becomes very slow in the later stages with an apparent Avrami exponent lower than 1. The assumption that PVA crystallites are the small entities that form at low temperatures in the unfrozen liquid microphase is in agreement with the fact that the size of the crystalline aggregates in the gels obtained by cryogenic treatments are always very small ( $\sim 3\text{--}4\text{ nm}$ ) and the degree of crystallinity remains below 2%

even upon storing the solutions at low temperatures for long time.<sup>12</sup>

**Acknowledgment.** We thank the Centro di Competenza “Nuove Tecnologie per le Attività Produttive” Regione Campania P.O.R. 2000–2006 Misura 3.16 and the Institut für Festkörperforschung of Jülich for provision of beam time. We thank Dr. Vitaly Pipich for valuable support at the KWS2 instrument and Dr. Rosa Ricciardi for help during measurements.

## References and Notes

- (1) (a) Hassan, C. M.; Peppas, N. A. *Adv. Polym. Sci.* **2000**, *153*, 37. (b) Lozinsky, V. I. *Russ. Chem. Rev.* **1998**, *67*, 573. (c) Lozinsky, V. I.; Galaev, I. Y.; Plieva, F. M.; Savina, I. N.; Jungvid, H.; Mattiasson, B. *Trends Biotechnol.* **2003**, *21*, 445.
- (2) (a) Peppas, N. M. *Makromol. Chem.* **1975**, *176*, 3433. (b) Stauffer, S.; Peppas, N. A. *Polymer* **1992**, *33*, 3932.
- (3) Lozinsky, V. I.; Damshkaln, L. G. *J. Appl. Polym. Sci.* **2000**, *77*, 2017.
- (4) Keller, A. *Faraday Discuss.* **1995**, *101*, 1.
- (5) Komatsu, M.; Takashi, T.; Miyasaka, K. *J. Polym. Sci., Part B: Polym. Phys.* **1986**, *24*, 303.
- (6) Tanaka, T.; Sislow, G.; Ohmine, I. *Phys. Rev. Lett.* **1979**, *42*, 1556.
- (7) Takeshita, H.; Kanaya, T.; Nishida, K.; Kaji, K. *Macromolecules* **1999**, *32*, 7815.
- (8) de Gennes, P.-G. *Scaling Concepts in Polymer Physics*; Cornell University Press: Ithaca, New York, 1979.
- (9) Willcox, P. J., Jr.; Howie, D. W., Jr.; Schmidt-Rohr, K.; Hoagland, D. A.; Gido, S. P.; Pudjijanto, S.; Kleiner, L. W.; Venkatraman S. *J. Polym. Sci., Part B: Polym. Phys.* **1999**, *37*, 3438.
- (10) Ricciardi, R.; Mangiapia, G.; Lo Celso, F.; Paduano, L.; Triolo, R.; Auriemma, F.; De Rosa, C.; Lauprêtre, F. *Chem. Mater.* **2005**, *17*, 1183.
- (11) Hassan, C. M.; Peppas, C. M. *Macromolecules* **2000**, *33*, 2472.
- (12) Ricciardi, R.; Auriemma, F.; De Rosa, C.; Lauprêtre, F. *Macromolecules* **2004**, *37*, 1921; Ricciardi R.; Auriemma F.; Gaillet, C.; De Rosa, C.; Lauprêtre, F. *Macromolecules* **2004**, *37*, 9510.
- (13) Bunn, C. W. *Nature (London)* **1948**, *161*, 929.
- (14) See for instance: Rubinstein, M.; Colby, R. H. *Polymer Physics*; Oxford University Press: New York, 2003.
- (15) Nagy, D. J. *Am. Lab.* **2003**, *35*, 38.
- (16) Emmerling, A.; Petricevic, R.; Beck, A.; Wang, P.; Scheller, H.; Fricke, J. *J. Non-Cryst. Solids* **1995**, *185*, 240.
- (17) Porod, C. In *Small Angle X-ray Scattering*; Glatter, O., Kratky, O., Eds; Academic Press: New York, 1982; p 17.
- (18) Wunderlich, B. *Macromolecular Physics, Crystal Melting*; Academic Press: New York, 1980; Vol. 3.
- (19) Grebowicz, J.; Cheng, S. Z. D.; Wunderlich, B. *J. Polym. Sci., Part B: Polym. Phys.* **1986**, *24*, 675.
- (20) Cheng, S. Z. D. *Macromolecules* **1988**, *21*, 2475.

MA061955Q